JOURNAL OF MATERIALS SCIENCE 26 (1991) 155–162

Microwave induced plasma processing of nuclear waste calcines

J.-G. PARK, D. C. LYNCH, S. H. RISBUD*
Department of Materials Science and Engineering, and Arizona Materials Laboratory, University of Arizona, Tucson, Arizona 85721, USA

Microwave induced plasma processing was used to sinter synthetic Idaho Chemical Processing Plant (ICPP) alumina and zirconia based high level nuclear waste calcines in a nitrogen atmosphere. The microwave densification behaviour of these nuclear waste calcines was observed parallel with identification of the phases formed after sintering. Sintered densities of $> 3.20\ g\,cm^{-3}$ were obtained within 10 min of microwave sintering of pure calcines. Glass frit containing calcines showed lower sintering densities ($< 2.0\ g\,cm^{-3}$) due to reactions between the frit and volatile substances in both zirconia based and alumina based calcines; prior removal of frit volatiles increased the sintered density. Phases formed in the microwave sintered calcines were identified by X-ray diffraction.

1. Introduction

Ceramic nuclear waste forms have advantages for the immobilization of high level waste (HLW) not found with glass, namely, greater thermodynamic stability, better heat resistance, high waste loading and significant volume reduction. Knecht and co-workers [1] have shown that ceramic waste forms with waste loadings of 60 to 85 wt %, and near theoretical density, yield HLW volume reductions of up to 60%, a significant finding in terms of the useful life of a disposal site, and the number of such facilities which will be necessary to meet the need for storage of nuclear waste.

Several methods have been investigated to immobilize nuclear wastes in the form of glass, glass–ceramics, and ceramics [2–4]. The major advantage of glass-containing ceramic forms over crystalline ceramics is their ability to preferentially accommodate elements such as boron, sodium and caesium in a relatively insoluble high silicon amorphous phases without degrading any of the properties of the crystalline phase [5]. A critical step in processing any waste ceramic form is the ability to achieve high densities in short time frames. Thus, sintering, hot pressing, and hot isostatic pressing (HIP) have all been used to densify ceramics for nuclear waste disposal. More recently, microwave induced plasma (MIP) processing has been used for the densification of various ceramics. Considerable interest has been shown in the rapid heating rates achieved with plasma and in the high densities achieved in short processing times with single phase materials [6–8].

In the present work we have examined the feasibility of using microwave induced plasma for densification of synthetic Idaho Chemical Processing Plant (ICPP) nuclear waste calcines. The densification behaviour, microstructure, and phases formed in sintered calcines (with and without frit addition) were investigated.

2. Background

2.1. Microwave plasma sintering

Sintering of ceramic oxides (e.g. Al_2O_3 and MgO) has been shown to be greatly accelerated by heating in microwave plasmas rather than by conventional furnace heating [9–11]. Bennett *et al.* [9] densified Al_2O_3 compacts in air at temperatures of 1300 to 1700 °C and demonstrated a significantly higher densification in plasma sintered pellets. Cordone and Martinsen [12] sintered Al_2O_3 rods in a d.c. glow discharge plasma and observed bulk densities as high as 96% of theoretical in < 5 min at approximately 1370 °C. Johnson and Rizzo [13] rapidly sintered β''-Al_2O_3 in a radio frequency inductively coupled plasma and reported densities of $> 98\%$ of theoretical. Kim and Johnson [6] densified tubes and rods of MgO-doped Al_2O_3 to theoretical densities in 15 and 25 sec. Kemer and Johnson [7] optimized the sintering behaviour of MgO-doped Al_2O_3 rods and observed 99.9% densification within 10 min of sintering in a microwave plasma.

A direct consequence of the rapid heating rates ($> 100\ °C\,sec^{-1}$) and densification observed in plasma heating of ceramics is the greatly reduced grain size (4 to 10 μm) in comparison with conventionally sintered samples (50 to 150 μm). The smaller grain size in plasma processed samples result from early densification by grain boundary and lattice diffusion before surface diffusion mechanisms can significantly coarsen the microstructure. An equally significant and practical aspect of reduced grain sizes permitted by microwave plasma sintering is the higher mechanical strength in the sintered bodies and possibly increased

* Present address: Department of Mechanical, Aeronautical and Materials Engineering, University of California, Davis, CA 95616, USA.

0022–2461/91 $03.00 + .12

hardness, corrosion and leaching resistance due to the close to ideal ceramic structure synthesized.

2.2. Chemical tailoring of nuclear waste

Sintering of unmodified nuclear waste does not yield a satisfactory ceramic. High sintering temperatures are required and these high sintering temperatures, in turn, volatilize Cs, Ru, Sb and Te [14–16]. In addition, sintering of unmodified wastes yield undesirable phases. For example, much of the caesium reacts with molybdenum to form water soluble caesium molybdates [14].

To solve that problem it has been theorized that tailored ceramic waste forms could be developed which incorporate all radwaste components into phases which are (1) insoluble, (2) readily densified, (3) incorporate high waste loads, (4) are thermodynamically compatible with each other, and (5) do not suffer significant radiation damage. A satisfactory solution to items 1, 4 and 5 would ensure long term stability and immobilization of radwaste, while a solution to items 2 and 3 would minimize both the volume of material to be stored and the cost of permanent containment facilities.

Just what is involved in tailoring ceramic waste forms can be deduced from an evaluation of mineral formulas [14, 17]. That analysis reveals that ceramic structures are likely to contain a minimal number of either cations or anions. While examples abound of minerals containing two cations or anions, it is rare to find structures containing three, four or more different cations or anions. It is, therefore, not practicable to create a ceramic material (excluding glass) consisting of a single phase containing all elements present in radwaste [14]. Typical ceramic waste forms must contain several phases with broad compositional ranges to incorporate all waste species.

Examples of tailoring include additions of Ca, Sr, Al and Si (as oxides) to adjust the overall composition of a simulated (nonradioactive) waste to yield favourable phase development [18]. Calcia and silica additions assist in incorporating lanthanons into an apatite-structured phase, while rubidium and caesium (which do not enter into the structure of other phases) are conditioned by additions of alumina and silica to form pollucite ((Rb, Cs) $AlSi_2O_6$). Both structures are stable at elevated temperatures.

Another approach to immobilization of a wide range of ions has been the development of "SYNROC". The SYNROC concept arose as a result of observations on the durability of those natural minerals which are capable of containing quantities of principal components of radwaste [19]. Synthetic equivalents of many of these minerals can be prepared by sintering. Through substitution of ions, the SYNROC approach utilizes these mineral structures as hosts for incorporation of radwaste.

3. Experimental procedures

Rod shaped specimens were prepared from simulated zirconia and alumina based nuclear waste calcines and glass frit provided by the Idaho Chemical Processing Plant (ICPP). The composition of the calcines and the frit (ICPP number 127) are shown in Tables I and II. The particle size of the as-received calcines was 220 μm. The calcines were ground in a shatter box for 3 min and then sieved to minus 200 mesh. The resulting powders were mixed with frit in the appropriate proportions and then cold pressed at 68.9 MPa to form rods 0.625 cm in diameter and 1.8 cm in length.

TABLE I Elemental analysis of calcines

Element	Zirconia based calcine – 5B (wt %)	Alumina based calcine – 9B (wt %)
Al	17.83	35.32
B	0.73	0.41
Ca	22.56	5.92
Cd	0.37	0.10
Cs	0.01	< 0.01
K	0.09	0.01
Na	0.64	0.30
Sr	0.11	0.02
Zr	12.56	3.64

TABLE II Composition of glass frit used

Compound	Content (wt %)
SiO_2	70.3
Na_2O	12.8
Li_2O	6.2
B_2O_3	8.5
CuO	2.1

The apparatus used for microwave plasma induced sintering is represented schematically in Fig. 1. A Gerling's GL 102 generator containing a magnetron operating at 2450 MHz was used to supply the microwave energy. The power from the generator could be varied from 0 to 3.0 kW, and was delivered to the applicator by a wave guide. The applicator includes an aluminium tube, which connects to the wave guide, and a silica tube. The silica tube was placed inside the aluminium tube, and, because it is evacuated, effectively confines the plasma. A number of small holes were drilled into the aluminium applicator through which air was blown to cool the silica tube used to

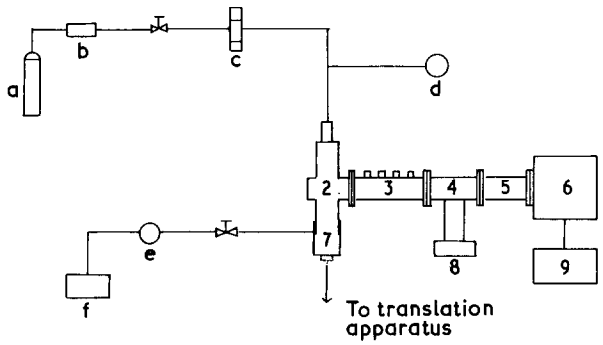

Figure 1 Schematic of microwave induced plasma apparatus. (a) Gas tank, (b) gas regulator, (c) flow meter, (d) vacuum pressure gauge, (e) trap, (f) vacuum pump. (1) Quartz tube, (2) wave guide applicator, (3) tuner, (4) directional coupler, (5) 3-port circulator, (6) microwave generator, (7) head attachment, (8) forward and reflected power meter, (9) control unit.

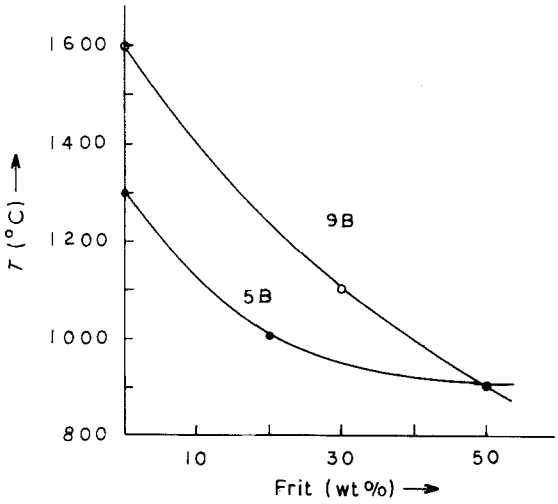

Figure 2 Effect of frit content on effective fusion temperature of calcines.

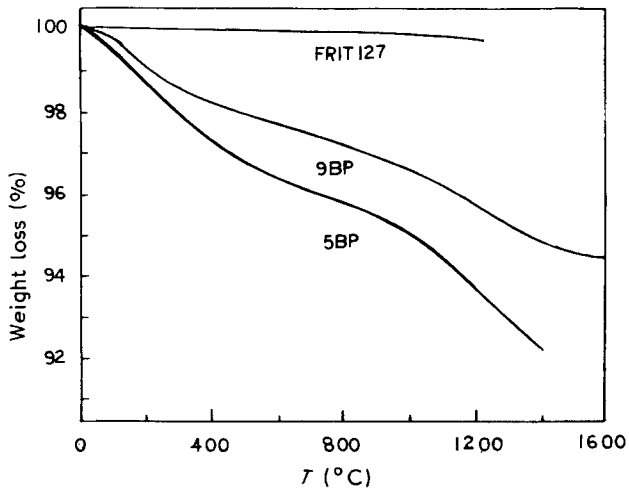

Figure 3 Cumulative weight loss associated with volatiles as a function of temperature.

contain plasma. A larger hole, approximately 1.25 cm in diameter, was made through applicator at the right angle to the wave guide so that an optical pyrometer could be used to monitor the temperature of the solid specimen.

A typical experiment was begun by placing the rod shaped specimen in the boron nitride holder which itself was attached to an alumina rod. The alumina rod was connected to a device which provided rotation of the specimen. The plasma was ignited by reducing the pressure to 133 Pa (1 torr) and introducing nitrogen flow as the power was turned on. After a plasma was established both the power level and the pressure in the tube were adjusted to the desired setting.

Microstructures of cross sections of plasma sintered rods were observed using scanning electron microscopy. Densities of sintered specimens were determined using the Archimedes method. Due to the presence of volatile species in the calcines, thermogravimetric analyses (TGA) were performed to measure the weight loss of the calcines and frit as a function of temperature. The phases formed after plasma sintering were identified using X-ray diffraction.

4. Results and discussion

4.1. Effective fusion temperature and weight loss

The borosilicate glass frit (ICPP-127) has been previously examined as an additive in hot isostatic pressing of nuclear waste calcines [5]. The use of frit (a mixture of various compounds in the form of glass powder) to form desirable phases in glass–ceramics is well known and the addition of frit to the calcines does alter their effective fusion temperature. Both the zirconia and alumina based calcines and frit, were heated in a furnace to ascertain their effective fusion temperature; the effective fusion temperature is defined as that temperature at which there was substantial coalescence between particles of frit and calcines as determined with optical microscopy. The results, shown in Fig. 2, were used to define the maximum sintering temperatures employed in subsequent experiments. Fig. 2 shows that the maximum sintering temperature that could be employed with the zirconia and alumina based calcines were 1300 and 1600 °C, respectively. Frit addition to the calcines reduced the effective fusion temperature of the admixtures to ~ 920 °C for both calcines that were mixed equally by

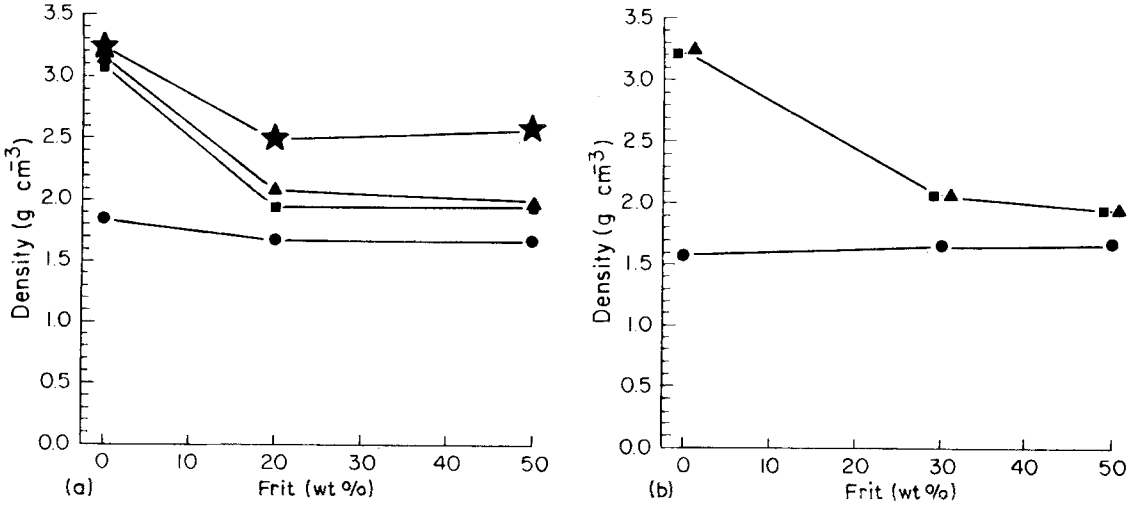

Figure 4 Comparison of densities achieved with the various heating schedules: (a) zirconia based calcines, (b) alumina based calcines. (●) Green density, (■) sintered density, (▲) pre-heating, (★) pretreating at 1100 °C.

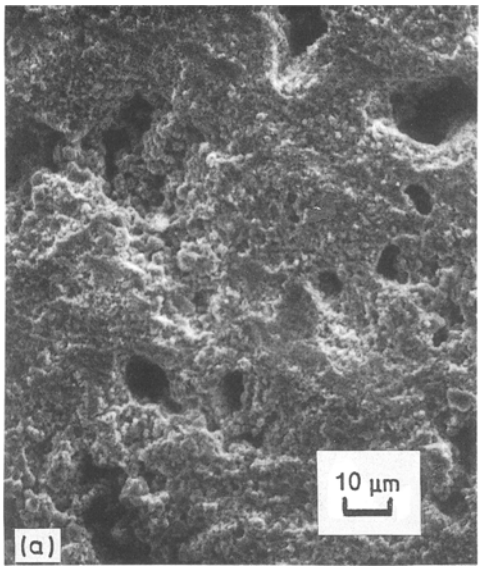

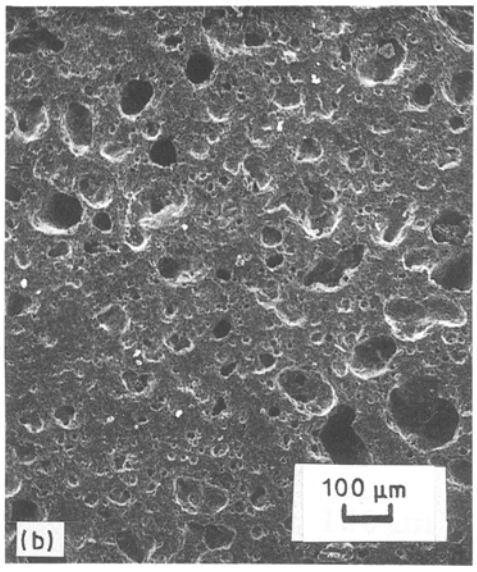

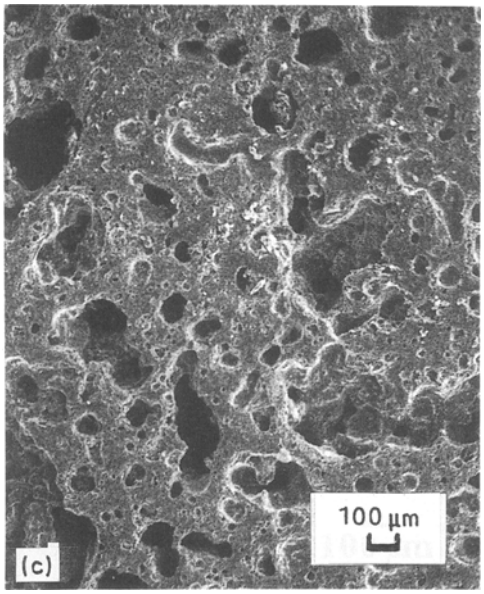

Figure 5 Internal structure of zirconia based calcines sintered at temperature below the effective fusion temperature: (a) 5BF, (b) 5BF20 and (c) 5BF50. See Table IV for specific conditions.

weight with frit. The fusion temperature of the frit alone was found to be $\sim 600\,^{\circ}C$.

TGA results of the weight loss upon heating are shown in Fig. 3 where the weight of the specimen as a function of temperature is shown as a per cent of the initial weight. Both calcines exhibited significant weight loss upon the commencement of heating due to the presence of hydrated species. The calcines continued to lose weight at elevated temperatures indicating the presence of other volatile species in the calcines. The zirconia based calcine exhibited the largest amount of weight loss because of the presence of larger concentrations of boron, sodium, potassium and caesium in these calcines. These elements have been reported [20] to be present in nuclear waste when heated to temperatures above 800 °C.

4.2. Densification by MIP

The green densities of the specimens prior to MIP sintering are shown in Fig. 4 as a function of the weight per cent of glass frit in the specimen. The green densities range from 1.5 to 2.0 $g\,cm^{-3}$, the highest density being observed in the specimen with no frit addition. On the whole there was little variation in the green density, although the addition of frit into calcines appeared to inhibit densification during subsequent MIP sintering. Scanning electron microscopy of the MIP sintered specimens revealed a sintered matrix surrounding numerous pores (as shown in Figs 5, 6 and 7). This information, coupled with knowledge of the effective melting points of the calcines and glass frit, suggests that sintering of the calcines in the MIP is hindered by trapping of evolved gases during the fusion of the glass frit. In order to verify this possibility both pure calcines and calcines mixed with frit were subjected to various heating schedules designed to establish the importance of frit and evolved gases in the MIP sintering process. The heating schedules involved: (a) MIP sintering specimens at temperatures based on their effective fusion temperatures; (b) pre-heating the specimens to expel gases before MIP sintering at the effective fusion temperature; (c) pretreating the calcines at 1100 °C in a box furnace for

TABLE III Pre-heating and sintering temperatures

Specimen	Pre-heat temperature (°C)	Sintering temperature (°C)
Zirconia based calcines[a]		
5BF	900	1300
5BF20	700	1000
5BF50	700	900
Alumina based calcines[a]		
9BF	1100	1600
9BF30	900	1100
9BF50	700	950

[a] Terminology: 5B(or 9B)F: 100% zirconia (or alumina) based calcine sample, 5B(or 9B)F20 (or 30): zirconia (or alumina) based sample mixed with 20(or 30)wt % frit, etc.

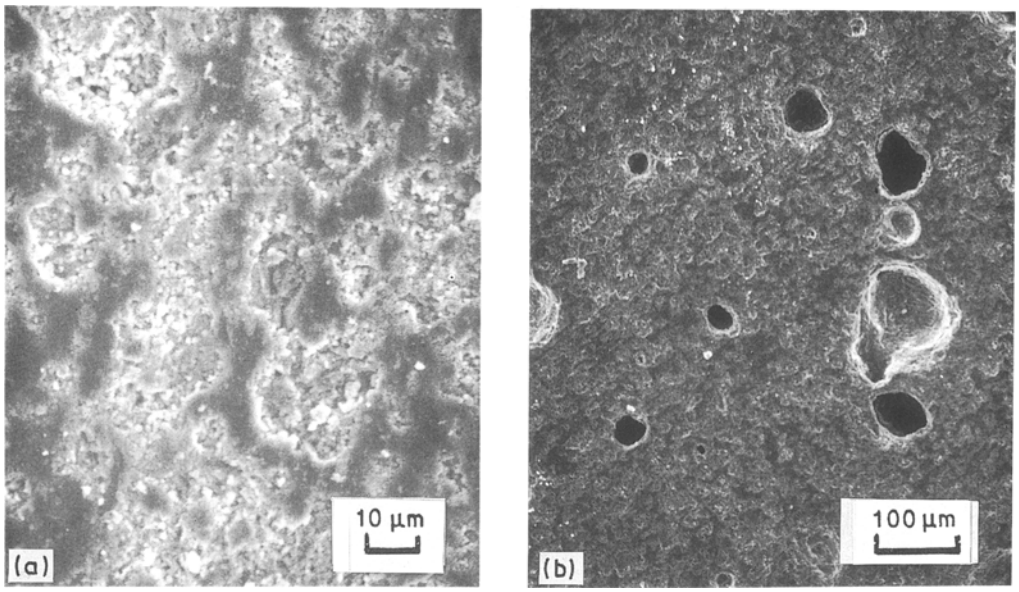

Figure 6 Internal structure of zirconia based calcines sintered at temperature below the effective fusion temperature after pretreatment at 1100 °C for 12 h: (a) 5BF, (b) 5BF20 and (c) 5BF50. See Table IV for specific conditions.

12 h, grinding to minus 200 mesh, and then mixing the calcines with frit before MIP sintering at the effective fusion temperature. The results of these experiments are tabulated in Tables III, IV and V, respectively. Again, the decline in the ultimate density with frit additions is also associated with reduction in the effective fusion temperature.

The preheating temperatures employed ranged from 700 to 1100 °C. For specimens containing frit the temperature range was significantly less, ranging only between 700 to 900 °C. TGA results indicated that at 700 °C the zirconia based calcines lost ~ 4 wt % while the alumina based calcine lost only 2 wt %. At 900 °C the losses were 4.5 and 3 wt %, respectively. The results in Fig. 4a and b indicate that pre-heating the specimens has a slight impact on the zirconia based calcines but almost no effect on the alumina based calcines.

The calcines that were pretreated at 1100 °C before being mixed with frit yielded substantially higher sintered densities than other calcines sintered with frit. Those specimens sintered without frit achieved the greatest density. As shown by the weight loss data not all volatiles were evolved at 1100 °C. The sintering

TABLE IV Experimental MIP processing conditions and results for Zirconia based calcines

	5BF	5BF	5BF	5BF20	5BF20	5BF20	5BF50	5BF50	5BF50
Heat treatment									
1. Pretreatment temperature for calcines (°C)[a]	NA	NA	1100	NA	NA	1100	NA	NA	1100
2. Sintering process									
(a) Preheating temperature (°C)	NA	900	NA	NA	700	NA	NA	700	NA
(b) Sintering temperature (°C)	1300	1300	1300	1000	1000	1000	900	900	900
P_N (KPa)	4.4	1.1, 4.4	4.4	1.1	1.1, 1.1	1.1	1.1	1.1, 1.1	1.1
Sintering time (min)	10	10, 10	10	10	10, 10	10	10	10, 10	10
Forward power (kW)		0.20			0.10			0.10	
	0.60	0.60	0.60	0.30	0.30	0.30	0.15	0.15	0.15
Reflected power (kW)	0.02	0.02	0.02	0.02	0.02	0.02	0.02	0.01	0.01
Silica tube diameter (mm)	22	22	22	22	22	22	22	22	22
Rotational speed (r.p.m.)	22	22	22	22	22	22	22	22	22
Die press (MPa)	68.9	68.9	68.9	68.9	68.9	68.9	68.9	68.9	68.9
Green density (g cm^{-3})	1.85	1.85	1.85	1.67	1.67	1.67	1.67	1.67	1.67
Final density (g cm^{-3})	3.08	3.15	3.23	1.95	2.09	2.50	1.95	2.00	2.58

[a] Held at temperature for 12 h in a box furnace.

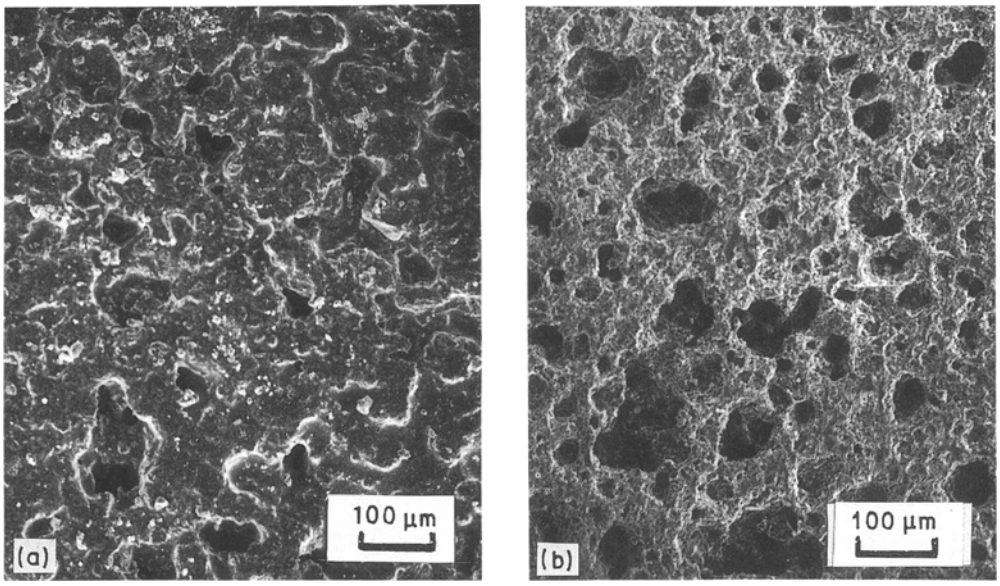

Figure 7 Internal structure of alumina based calcines sintered at temperature below the effective fusion temperature: (a) 9BF, (b) 9BF30 and (c) 9BF50. See Table V for specific conditions.

temperature employed with zirconia based calcines mixed with 50 wt % frit (5BF50) was 900 °C and the sintering temperature employed with specimens mixed with 20 wt % frit (5BF20) was 1100 °C. Gas evolution from the pretreated calcines at the lower sintering temperatures may not be anticipated because both temperatures are below the pretreatment temperature. In addition the energetic electrons and radicals in the plasma, and the very presence of the frit, may yield volatiles. Those gases can be trapped by molten frit resulting in pores as shown in Fig. 6b and c.

The weight loss data shown in Fig. 3, and MIP sintering densities in Fig. 4, coupled with the micrographs in Figs 5 to 7, clearly support the idea that the glass frit, which fuses at ~ 600 °C, traps evolved gases and leads to porosity in the sintered calcines.

4.3. Phase(s) identification

X-ray diffraction was used to identify phases in both the as-received calcines and MIP sintered specimens, and the results are shown in Figs 8 and 9. The glass frit was X-ray amorphous while the as-received zirconia based calcine showed the presence of ZrO_2 and CaF_2. Sintering of calcines, without frit, at 1300 °C still yields strong X-ray traces for CaF_2, but significant reduction in the ZrO_2 peaks appears to be associated with new peaks for $CaZrO_3$. The MIP sintered sample

TABLE V Experimental MIP processing conditions and results for alumina based calcines

	9BF	9BF	9BF30	9BF30	9BF50	9BF50
Heat treatment						
1. Pretreatment temperature for calcines (°C)*	NA	NA	NA	NA	NA	NA
2. Sintering process						
(a) Preheating temperature (°C)	NA	1100	NA	900	NA	700
(b) Sintering temperature (°C)	1600	1600	1100	1100	1100	1100
P_N (KPa)	16	4.4, 16	4.4	2.0, 4.4	2.0	2.0, 2.0
Sintering time (min)	10	10	10	10	10	10
Forward power (kW)	0.6	0.3, 0.6	0.3	0.2, 0.3	0.2	0.1, 0.2
Reflected power (kW)	0.02	0.02	0.02	0.02	0.02	0.02
Silica tube diameter (mm)	22	22	22	22	22	22
Rotational speed (r.p.m.)	22	22	22	22	22	22
Die press (MPa)	68.9	68.9	68.9	68.9	68.9	68.9
Green density ($g\,cm^{-3}$)	1.57	1.57	1.65	1.65	1.67	1.67
Final density ($g\,cm^{-3}$)	3.21	3.24	2.06	2.07	1.95	1.95

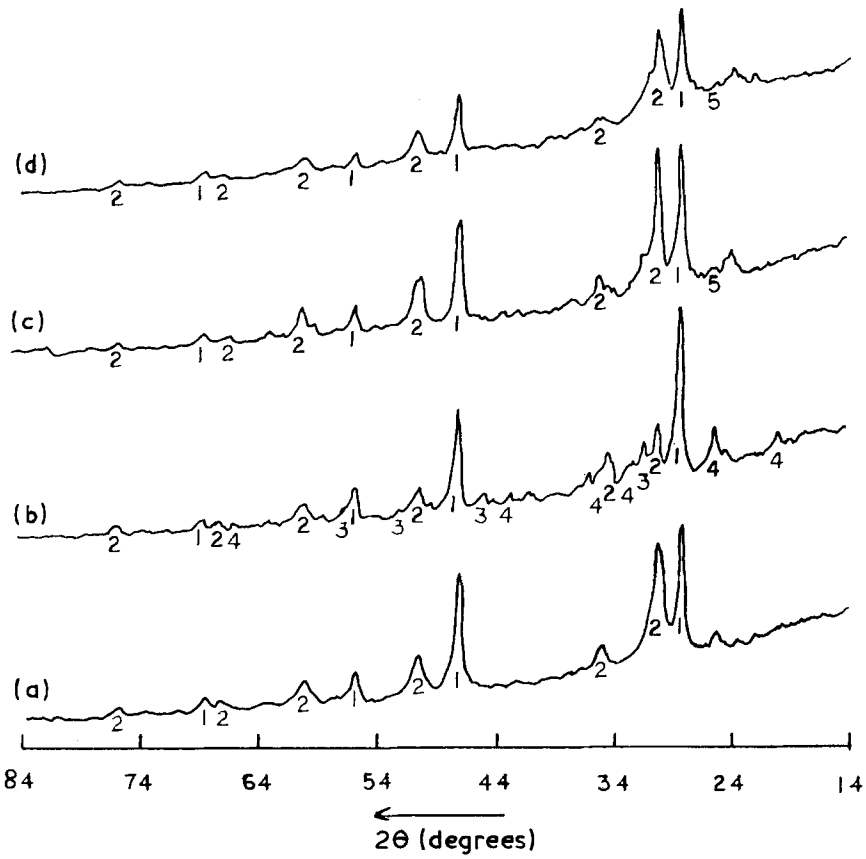

Figure 8 X-ray diffraction peaks for (a) 5BF green sample, (b) 5BF sintered at 1300 °C, (c) 5BF20 sintered at 1000 °C and (d) 5BF50 sintered at 900 °C. (1) CaF_2, (2) ZrO_2, (3) $CaZrO_3$, (4) $2Al_2O_3 \cdot CaO$, (5) $ZrSiO_4$.

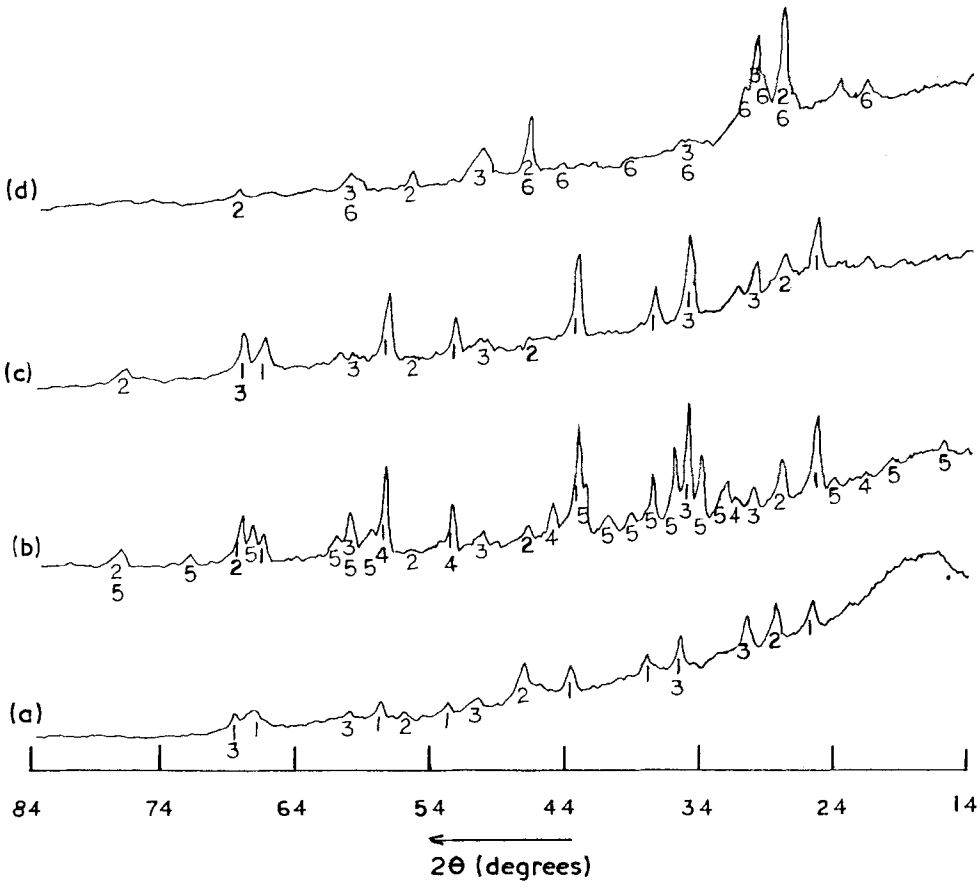

Figure 9 X-ray diffraction peaks for (a) 9BF green sample, (b) 9BF sintered at 1600 °C, (c) 9BF30 sintered at 1100 °C and (d) 9BF50 sintered at 950 °C. (1) Al_2O_3, (2) CaF_2, (3) ZrO_2, (4) $CaZrO_3$, (5) $6Al_2O_3 \cdot CaO$, (6) $Na_3KAl_4\ Si_4O_6$.

of the zirconia based calcine also showed X-ray peaks for $CaO \cdot 2Al_2O_3$.

The addition of frit to the zirconia based calcine led to the disappearance of the $CaO \cdot 2Al_2O_3$ phase and to an indication that some of the zirconium in the calcine reacts with silica in the frit. Overall, there appears to be little change in the crystalline phases present in the MIP sintered specimen and the original calcine.

In comparison with zirconia based calcines, frit addition played a larger role in the MIP sintering of the alumina based calcines. X-ray analyses for MIP sintered alumina based calcines, shown in Fig. 9, showed crystalline phases of Al_2O_3, CaF_2, ZrO_2, $CaZrO_3$, and $CaO \cdot 6Al_2O_3$. The frit reacts with the calcine during sintering and X-ray data on alumina based calcine sintered with 30 wt % frit showed peaks for only Al_2O_3, CaF_2 and ZrO_2. Increasing the frit content to 50 wt % resulted in the disappearance of Al_2O_3 and formation of the crystalline phase $Na_3KAl_4Si_4O_6$.

5. Summary and conclusions

1. Plasma induced sintering can be used to achieve rapid densification in the calcines, but not without significant drawbacks. Finely ground specimens of zirconia and alumina based calcines, with green densities of approximately 1.8 $g\,cm^{-3}$, were sintered to a density of 3.2 $g\,cm^{-3}$ within 10 min. While rapid sintering can be achieved with the pure calcines, the addition of glass frit to the specimens seems to significantly hinder the MIP sintering process.

2. The presence of glass frit in the specimen, and its interaction with volatiles emitted from the calcines, resulted in a significant decrease in the ultimate density of the specimens. Thermogravimetric analysis of the calcines and frit revealed that both calcines emit volatiles almost continuously as they are heated in the microwave plasma.

3. The X-ray diffraction results obtained in the present investigation indicate that little chemical reaction occurs between the glass frit and the zirconia based calcines. The glass frit was, however, found to react with the alumina in the calcines to produce a $Na_3KAl_4Si_4O_6$ crystalline phase.

Acknowledgement

This work is based on a MS thesis by J. G. Park. Support from the US Department of Energy through the Westinghouse Idaho Nuclear Company, Inc, is gratefully acknowledged.

References

1. D. A. KNECHT, J. R. BERRETH, N. A. CHIPMAN, H. S. COLE, B. A. STAPLES and W. B. KERR, Scoping Studies to Reduce ICPP High-Level Radioactive Waste Volumes for Final Disposal, paper presented at Waste Management. '86 Conference, Tucson, Arizona, March 1986.
2. P. A. TEMPEST, *Nuclear Technol.* **52** (1981) 415.
3. G. G. WICKS and W. A. ROSS, "Nuclear Waste Management", Vol. 8 (American Ceramic Society, Westerville, Ohio, USA, 1983) p. 272.
4. L. P. HATCH, *Am. Sci.* **41** (1953) 410.
5. A. B. HARKER and J. F. FLINTOFF, *J. Am. Ceram. Soc.* **68** (3) (1985) 159.
6. J. S. KIM and D. L. JOHNSON, *J. Am. Ceram. Soc. Bull.* **62** (1983) 620.
7. E. L. KEMER and D. L. JOHNSON, *ibid.* **64** (1985) 1132.
8. K. KIJIMA, in Proceedings of the 7th International Symposium on Plasma Chemistry, Vol. 2, Eindhoven University of Technology, Eindhoven, Netherlands, July, 1985, edited by C. J. Timmermans (Elsevier Science, Amsterdam) p. 662.
9. C. E. G. BENNETT, N. A. McKINNON and L. S. WILLIAMS, *Nature* **217** (1968) 1287.
10. C. E. G. BENNETT and N. A. McKINNON, "Kinetics of Reactions in Ionic Systems" (Plenum Press, New York, 1969) p. 408.
11. D. L. JOHNSON, V. A. KRAMB and D. C. LYNCH, "Emergent Process Methods for High-Technology Ceramics", Vol. 17 (Plenum Press, New York, 1984) p. 207.
12. L. G. CORDONE and W. E. MARTINSEN, *J. Am. Ceram. Soc.* **55** (7) (1972) 380.
13. D. L. JOHNSON and R. A. RIZZO, *ibid.* **59** (4) (1980) 467.
14. F. P. GLASSER, *Brit. Ceram. Soc. J.* **84** (1985) 1.
15. G. W. WILDS, "Vaporization of Semi-Volatile Components from Savannar River Plant Waste Glass", Report No. DP 1504, Du Pont de Nemours (E.I.) and Co., Aiken, SC. Savannah River Laboratory, August 1978.
16. W. G. GARY, "Volatility of a Zinc Borosilicate Glass Containing Simulated High-Level Radioactive Waste", Report No. BNWL- 2111, Battelle Pacific Northwest Labs, Richland Wash., October 1976.
17. L. F. GRANTHAM and J. F. FLINTOFF, in Proceedings of the Symposium on High Temperature Materials Chemistry, Denver Colorado, 1981, edited by D. D. Cubicciotti and D. L. Hildenbrand, p. 167.
18. G. J. McCARTHY, "Advanced Waste Forms Research and Development", Report No. COO-2510-15, Pennsylvania State University, University Park, Pennsylvania, August 1979.
19. F. J. RYERSON, C. L. HOENIG and G. S. SMITH, in Proceedings of the Symposium on High Temperature Materials Chemistry Denver Colorado, 1981, edited by D. D. Cubicciotti and D. L. Hildenbrand (Electrochemical Society, Pennington, New Jersey, USA) p. 144.
20. W. J. GARY, *Radioactive Waste Management* **1** (1980) 147.

Received 13 November
and accepted 1 December 1989